Journal of Biomedical Optics 8(3), 534–544 (July 2003)

Near-infrared thermo-optical response of the localized reflectance of intact diabetic and nondiabetic human skin

Shu-jen Yeh
Omar S. Khalil
Charles F. Hanna
Stanislaw Kantor
Abbott Laboratories. Diagnostics Division
D-9NL AP20
100 Abbott Park Rd
Abbott Park, Illinois 60064-6015
USA
E-mail: shujen.yeh@abbott.com

Abstract. We observed a difference in the thermal response of localized reflectance signal of human skin between type 2 diabetics and nondiabetics. We investigated the use of this thermo-optical behavior as the basis for a noninvasive method for the determination of the diabetic status of a subject. We used a two-site temperature differential method, which is predicated upon the measurement of localized reflectance from two areas on the surface of the skin. Each of these areas is subjected to a different thermal perturbation. The response of localized reflectance to temperature perturbation was measured and used in a classification algorithm. We used a discriminant function to classify subjects as diabetic or nondiabetic. In a prediction set of twenty-four noninvasive tests collected from six diabetic and six nondiabetic subjects, the sensitivity ranged between 73 and 100%, and the specificity ranged between 75 and 100%, depending on the thermal conditions and the probe–skin contact time. The difference in the thermo-optical response of the skin of the two groups is explained in terms of a difference in the response of cutaneous microcirculation, which is manifested as a difference in the near-infrared light absorption. Another factor is the difference in the temperature response of the scattering coefficient between the two groups, which may be caused by cutaneous structural differences induced by nonenzymatic glycation of skin protein fibers, and possibly by the difference in blood cell aggregation.
[DOI: 10.1117/1.1578641]

Keywords: diabetes; diabetic skin; near infrared; thermo-optical response; localized reflectance; discriminant function.

Paper JBO 02049 received Jul. 30, 2002; revised manuscript received Nov. 18, 2002; accepted for publication Jan. 3, 2003.

1 Introduction

There is growing interest in transcutaneous optical measurements for the noninvasive determination of glucose in human tissue, and the technologies used were recently reviewed.[1] In many reported studies, transmission or reflectance measurements were performed on diabetic and nondiabetic subjects. A change in their blood glucose concentration was induced. Multivariate analysis was used to generate calibration relationships between glucose change and optical signal. These measurements were performed at a constant temperature or at an uncontrolled temperature. In addition, these studies considered human skin to be a passive component in the optical measurement.[2,3] The possible differences in the physical and physiological properties of diabetic and nondiabetic skin, their effect on the optical signals, and the role of temperature were not considered. It is important to study the optical and thermal properties of human skin, especially that of diabetic subjects, because it acts as a window for the spectral measurements on human tissue.

It is well known that diabetes mellitus affects microcirculation and leads to microvessel complications such as neuropathy, retinopathy, and nephropathy. Laser Doppler flowmetry (LDF) studies showed impaired circulation in diabetic patients, which was manifested by a decrease in cutaneous blood flow and a difference in blood flow response to cooling or warming.[4–7] Vascular walls in the cutaneous microvasculature of diabetic patients were abnormally thick,[8] and blood vessels responded subnormally to heat, injury, and histamine.[9–11] Diabetic subjects exhibited differences from normal subjects in cutaneous blood flow,[10–12] elevated nailfold capillary pressure,[12] reduced maximal hyperemia,[13] impaired peripheral vasomotion,[14] response to contralateral cooling,[15] and skin microvascular regulatory response.[16] Also, different blood flow motion in patients with peripheral diabetic neuropathy was reported.[17] In addition, a set of skin structural effects was associated with diabetes. Differences in dermal collagen structure and in its X-ray diffraction patterns were attributed to glycation and cross-linking of cutaneous collagen fibers resulting from frequent hyperglycemic episodes in diabetics.[18–20]

The reported blood circulation and structural differences in the skin raise the possibility of a difference in skin localized reflectance in the visible and near-infrared range, and a difference in the response to thermal stimulation that is dependent

1083-3668/2003/$15.00 © 2003 SPIE

on the diabetic status of the subjects. Advantages of the localized reflectance measurement technique include simple and inexpensive instrumentation, simple manipulation, and minimum discomfort of subjects. The method incorporates both tissue and blood scattering, as well as light absorption by tissue and blood components. The LDF measurements yield mainly blood flow parameters.

Recently we studied the effect of temperature on the absorption and scattering coefficients of human skin.[21,22] We reported a reversible temperature effect on the absorption and scattering coefficients of intact human skin by measuring the temperature-modulated localized reflectance on the dorsal side of human forearms. *Ex vivo* human skin also exhibits a reversible temperature effect on the scattering coefficient.[23] We also reported the use of temperature changes for the noninvasive determination of hemoglobin.[24]

In this study we investigate temperature effect on the localized reflectance of the skin of diabetic and nondiabetic subjects measured between 590 and 935 nm. We examine the dependence of temperature-induced reflectance changes on the diabetic status of the subject. The wavelengths were selected to include deoxyhemoglobin at 590 nm, oxyhemoglobin at 660 nm, the water overtone absorption at 890 nm, and a deeper penetrating wavelength at 935 nm. These wavelengths allow monitoring of the combined change in blood circulation and change in light scattering by skin at different temperatures.

The purpose of this work is to determine if there is a measurable difference in the optical reflectance response of diabetic and nondiabetic skin to temperature perturbations. Second, we investigate if this difference can be used to classify diabetic and nondiabetic subjects. The results suggest a difference in the thermo-optical response between diabetic and nondiabetic skin and the ability to classify the two populations based on the temperature-induced localized reflectance measurements. The study was performed on a limited population, and a larger sample size is needed to establish the validity of this method for the classification of diabetic status and its potential use as a screening tool for diabetes.

2 Theoretical Background

The method is based upon measuring the temperature effect on localized reflectance signals at two neighboring sites on the human skin where each site is subjected to independent external temperature perturbations. The temperature perturbation consists of a set of programmed temperature-time events that are applied to the skin during the optical measurements. Localized reflectance is measured at skin site 1, where a temperature program involves cooling the skin at a given rate and for a given duration. The localized reflectance signals $R_{A1}(\lambda_i, r_j, T_k)$ and $R_{A1}(\lambda_i, r_j, T_l)$ at two time points corresponding to two temperature values are recorded. In these expressions, λ_i is the wavelength of light, r_j is the distance between the illumination fiber and a light collection fiber in contact with the skin. T_k and T_l are cutaneous temperatures attained after k seconds and l seconds of contact between the temperature-controlled optical probe and the skin. A1 and A2 designate the two measurement sites on the skin. Cooling has both physiological and optical effects. Cooling results in vasoconstriction, accompanied by decreased blood perfusion, which leads to decreased light absorption. Cooling also leads to a decrease in the scattering coefficient, which is an optical effect.[22,23] From the measured quantities we calculate the natural log of the ratio of the reflectance at the first site, for each wavelength, each source–detector distance, and different temperatures; $\ln\{R_{A1}(\lambda_i, r_j, T_l)/R_{A1}(\lambda_i, r_j, T_k)\}$, where T_l is at a time point later than T_k.

Simultaneously or sequentially, we performed a measurement at skin site 2, where the temperature program involves heating the skin. We measured $R_{A2}(\lambda_i, r_j, T_p)$ and $R_{A2}(\lambda_i, r_j, T_q)$ at two time points (p and q) corresponding to two temperature values. Heating also has both physiological and optical effects on skin. Heating results in vasodilation, which leads to increased blood perfusion and increased light absorption at the hemoglobin wavelengths. Heating also leads to an increase in the scattering coefficient of the skin, which is an optical effect.[22,23] From the measured quantities we calculate the value $\ln\{R_{A2}(\lambda_i, r_j, T_q)/R_{A2}(\lambda_i, r_j, T_p)\}$, where T_q is at a later time than T_p.

Since the change in temperature induces a small change in the reflectance over the range studied, the value of the natural logarithm can be expressed using the expansion $\ln(1\pm x) = \pm x$, where x is the fractional change in localized reflectance at λ_i and r_j. Thus, $\ln\{R_{A1}(\lambda_i, r_j, T_l)/R_{A1}(\lambda_i, r_j, T_k)\}$ is the temperature-induced fractional change in $R(\lambda_i, r_j)$ at site 1. Similarly, $\ln\{R_{A2}(\lambda_i, r_j, T_q)/R_{A2}(\lambda_i, r_j, T_p)\}$ is the temperature-induced change in $R(\lambda_i, r_j)$ at site 2. The quantities are also proportional to optical density changes induced by temperature.

The difference in the temperature-induced fractional change in the localized reflectance at two skin sites, ΔR_T, is expressed as

$$\Delta R_T = \ln\{R_{A1}(\lambda_i, r_j, T_l)/R_{A1}(\lambda_i, r_j, T_k)\} - \ln\{R_{A2}(\lambda_i, r_j, T_q)/R_{A2}(\lambda_i, r_j, T_p)\}. \quad (1)$$

The use of two independent temperature programs at two skin sites captures a wide range of skin thermal-optical responses. Taking the difference of the fractional changes at two sites minimizes the effects of skin–probe contact that are unrelated to temperature perturbation, such as fluid and tissue response to pressure. From theoretical analysis, Monte Carlo simulation, and experimental data,[21,25] it is known that localized reflectance is dependent on the scattering as well as absorption coefficients of the medium, and the scattering and absorption coefficients can be estimated from localized reflectance as a function of source–detector distance. Therefore, this ΔR_T for each λ_i and at various r_j incorporates both the change in the absorption coefficient, $\Delta\mu_a$, and the change in the scattering coefficient, $\Delta\mu_s'$, as a result of temperature changes. In general, the reflectance at a smaller distance is affected more by scattering than by absorption, and the reflectance at a larger distance is affected more by absorption. In a previous study,[22] we reconstructed from localized reflectance the absorption and scattering coefficients and their changes so that we could analyze the response of each property to thermal stimuli. In this study, which is oriented toward application, we use the fractional change in localized reflectance directly.

It is possible to relate the difference in the temperature-induced change in localized reflectance to the blood circula-

tion and structural differences in human skin that were mentioned in the introduction. The microcirculation response of skin to thermal stimuli differs between diabetic and nondiabetic subjects.[9,10,15] Recent reports on vasodilation induced through iontophoreses of chemical compounds showed differences in vasodilation between diabetic and nondiabetic subjects with diabetics having impaired dilation.[26,27] The difference affects blood volume change and blood flow velocity and can manifest itself as a difference in response of the absorption coefficient to thermal stimuli.

In addition, the combined structural effects of cutaneous fibers and red blood cells (RBCs) can lead to a difference in localized reflectance signals as a function of temperature. Differences between diabetic and nondiabetic red blood cell aggregation,[28–30] and differences in the mean refractive index of RBCs were reported.[31] Optical scattering of aggregated RBCs differs from that of the nonaggregated ones. The scattering of capillary RBCs and the refractive index mismatch between the cells and the plasma will vary with temperature and can contribute to the observed thermo-optical behavior of diabetic skin.

The reduced scattering coefficient μ_s' of a tissue was approximated by Graff et al.[32] It was expressed in terms of volume fraction of scattering centers as:[21]

$$\mu_s' = 2.46(\varphi/a)(2\pi a n_{\text{medium}}/\lambda)^{0.37}(M-1)^{2.09}, \quad (2)$$

where a is the average scatterer radius, φ $(=1.33\pi a^3\rho)$ is the effective volume fraction of scatterers, ρ is the number density of scattering centers in tissue; λi is the wavelength, and M is the ratio of the refractive index of scattering centers to that of the medium $(M = n_{\text{scatterer}}/n_{\text{medium}})$. Structural effects in tissue fibers associated with diabetes can affect the optical properties of diabetic skin. Studies on diabetic and nondiabetic skin revealed differences in the cutaneous collagen fibers.[18–20] Cross-linking of collagen fibers in skin can result in differentiation in a, ρ, or M. The presence of different ranges of scatterer radii for the diabetic group also leads to a difference in the effective volume fraction of the fibers; therefore $\varphi_{\text{diabetic}} > \varphi_{\text{nondiabetic}}$. In addition, a difference in the refractive index of the scatterer, $n_{\text{scatterer}}$, leads to a different refractive index mismatch M between the two populations, which can respond differently to temperature changes. As discussed later, the diabetic status determined from skin thermo-optical response was found to be independent of glucose concentration, which suggests that classification of the diabetic status is more dependent on $n_{\text{scatterer}}$ than on n_{medium}.

3 Experiments

3.1 *Instrument*

The schematic diagram of the temperature-controlled optical system used in this study is shown in Fig. 1. The instrument consists of a light source module, a human interface module, and a signal detection module. These three modules were interconnected through a branched optical fiber bundle. The light source module had four light-emitting diodes (LEDs) mounted in a circular holder, A. Light from the LEDs was focused onto the source tip, F, end of an illuminating fiber, G, by an objective lens, B (28-mm focal length RKE precision eyepiece, Edmund Scientific, part No. 30787). The LEDs

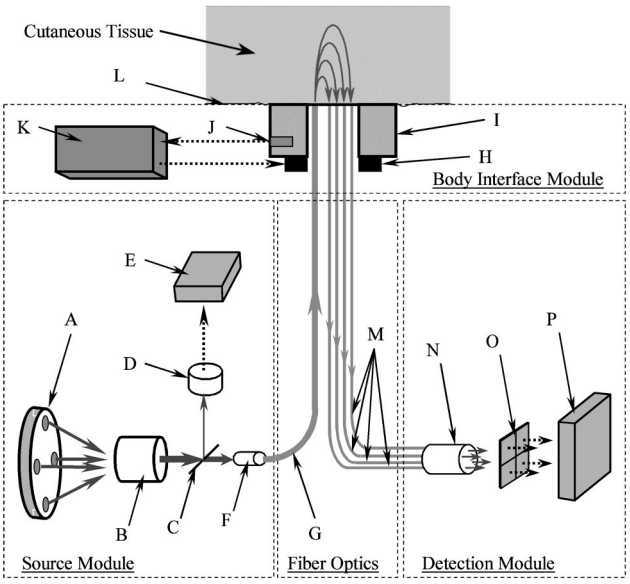

Fig. 1 Schematic diagram of the temperature-controlled optical system used in this study. A, circular holder for the LEDs; B, objective lens; C, beamsplitter; D, reference detector; E, amplifier for reference detector; F, source tip; G, source on illumination fiber; H, thermoelectric element; I, aluminum disk; J, thermocouple; K, temperature controller; L, skin surface; M, detection fibers; N, detection tip; O, quadrant photodiode; P, detection amplifiers. The dashed arrows depict an electronic signal and the solid arrows depict light beam directions.

were modulated by drive circuits (not shown), with each LED modulated at a different frequency. A portion of the light was diverted by a beamsplitter, C, and focused onto a silicon photodiode reference detector, D, which was amplified by amplifier, E, to generate a reference signal, which was used to correct for fluctuations in the intensity of the LEDs. A previously described optical system used up to six wavelengths and six source-detector distances that were varied sequentially though the use of stepper motor-controlled wheels.[22,24] This optical system uses a quadrant photodiode to allow simultaneous detection at four distances. Frequency modulating the LEDs and demodulating each detected signal allowed the simultaneous detection of four wavelengths.

The wavelengths and frequency at which each LED was modulated were 590 nm at 819 Hz, 660 nm at 1024 Hz, 890 nm at 455 Hz, and 935 nm at 585 Hz. The half-bandwidth of the first two LEDs was 25 nm and that of the last two was 50 nm. The power at the end of the illumination fiber was in the range of 1.4 to 5.0 μW for each LED, as measured by a power meter. The four photodiodes and the four LEDs were combined for the sixteen combinations of wavelengths and source–detector distances.

The output end of the illuminating fiber and the input ends of the light-collecting fibers were mounted in a common tip. All fibers were 400-μm diameter, low-OH silica. The distances between the source fiber and the light-collecting fibers were 0.44, 0.90, 1.21, and 1.84 mm, respectively. The common tip was situated at the center of a 2-cm diameter temperature-controlled disk, I, located in the human interface module. The disk temperature was controlled by a thermoelectric element, H. A thermocouple, J, embedded in the disk, provided feedback to the temperature controller, K (Marlow

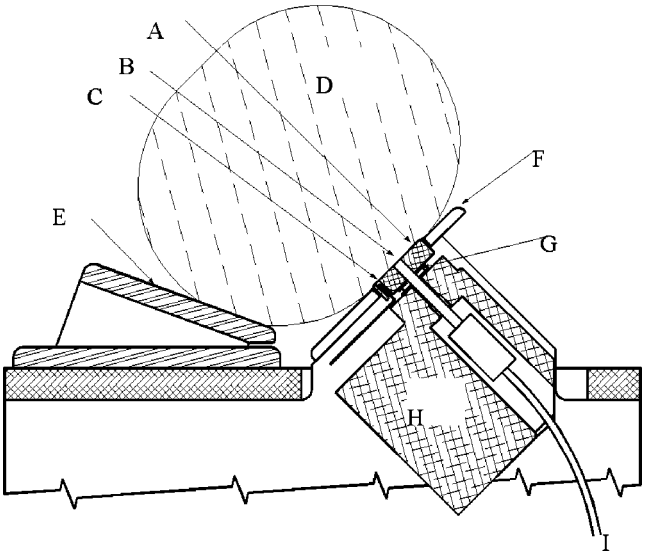

Fig. 2 Schematic drawing of the body interface. The interface is mounted on the armrest of a clinical reclining chair or is placed on a table. A, aluminum disk; B, common tip; C, thermocouple; D, cross-section of the arm; E, lower part of the armrest; F, upper part of the armrest; G, thermoelectric element; H, carriage carrying the detector head; I, fiber optic bundle to the sources and the detectors.

Industries, Dallas, Texas). The disk and common tip touched the skin surface, L. The light reemitted from the skin was collected by four detection fibers, M, and the output end of each fiber in the detection tip, N, was imaged onto one quadrant of a quad silicon photodiode detector, O (Hamamatsu S4349). The signal from each quadrant of the detector was separately amplified by transimpedance detection amplifiers, P, and measured by a Hewlett-Packard 3458A multimeter. The amplifiers and the frequency modulation drive boards were designed and built in house. The optical signals were collected every 3 s. Data were transferred to the computer every 30 s.

The signal from each quadrant of the detector represented light from one detector fiber, which corresponds to the signal at one source–detector distance. The signal at each modulation frequency corresponded to one wavelength.

The body interface module was mounted on a cradle (shown in Fig. 2), which was mounted on an arm of a standard clinical reclining chair (not shown). The subject sat in the chair with the forearm resting on the cradle. The optical probe located in the body interface module was pressed against the dorsal side of the subject's forearm at a constant force of 160 g (approximately 45 g/cm^2). A personal computer employed a LabView program (National Instruments, Austin, Texas) to manage data acquisition and set the temperature of the disk via the controller.

3.2 *Experimental Protocols*

We measured the localized reflectance signals at two sites on the dorsal side of the arms of the volunteers (Fig. 3). The two sites were not overlapping and were selected to be morphologically similar in such aspects as the absence of hair, closeness to bone, and appearance of veins. The company's institutional review board approved the test protocol, and each volunteer read and signed an informed consent form.

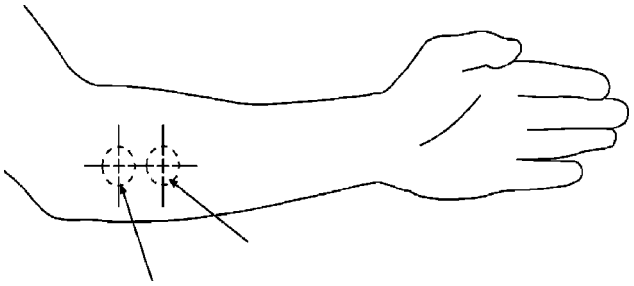

Fig. 3 Sketch of the two areas on the arm that are used as the optical measurement sites.

3.2.1 *Qualitative study*

Three experiments were conducted. The first experiment involved three subjects. Two of them were diabetic and the third was nondiabetic. The subjects were of similar build (a body mass index less than 27) and age. Each subject was tested three times. Reflectance measurements were performed on each subject using the following temperature perturbation program: The probe temperature at the first area was maintained at 38 °C for 300 s, then was gradually lowered to 22 °C over the course of 60 s, and then maintained at 22 °C for 120 s. Thus, temperature perturbation of the optical probe at this area changed from heating at 38 °C to cooling to 22 °C. The nine plots are shown in Fig. 4(A) and Sec. 4.1.

The test was immediately repeated on a second site on the skin. The probe temperature at this second site was maintained at 22 °C for 300 s, then was raised to 38 °C over the course of 60 s, and was maintained at 38 °C for 120 s. Data are plotted in Figs. 4(B) and 4(C) and discussed in Sec. 4.1.

A second experiment was also conducted on the same three subjects once, with the temperature perturbation program being the same at the two sites. Two of the three subjects were diabetic and the third was nondiabetic. The data are shown in Fig. 5.

In a third experiment, three additional volunteers of different age, ethnicity, and build (a body mass index greater than 32) than those tested in experiment 1 were tested using the same test protocol and temperature programs as in experiment 1. Each subject was tested twice. One subject was diabetic and two were nondiabetic. The combined data of the first group and the second group are shown in Fig. 6 and discussed in Sec. 4.1.

3.2.2 *Classification study with three sets of temperature programs*

Localized reflectance was measured at two sites on the dorsal side of the arms of the test subjects as in Sec. 3.2.1. The time of the skin–probe contact was reduced by half, resulting in two sequential measurements, each lasting 240 s. The time the skin was kept at a constant temperature was 30 s and the transition time for a temperature change was 180 s. Three different temperature limits were attempted and will be described later.

Nondiabetic subjects and type 2 diabetic subjects with a

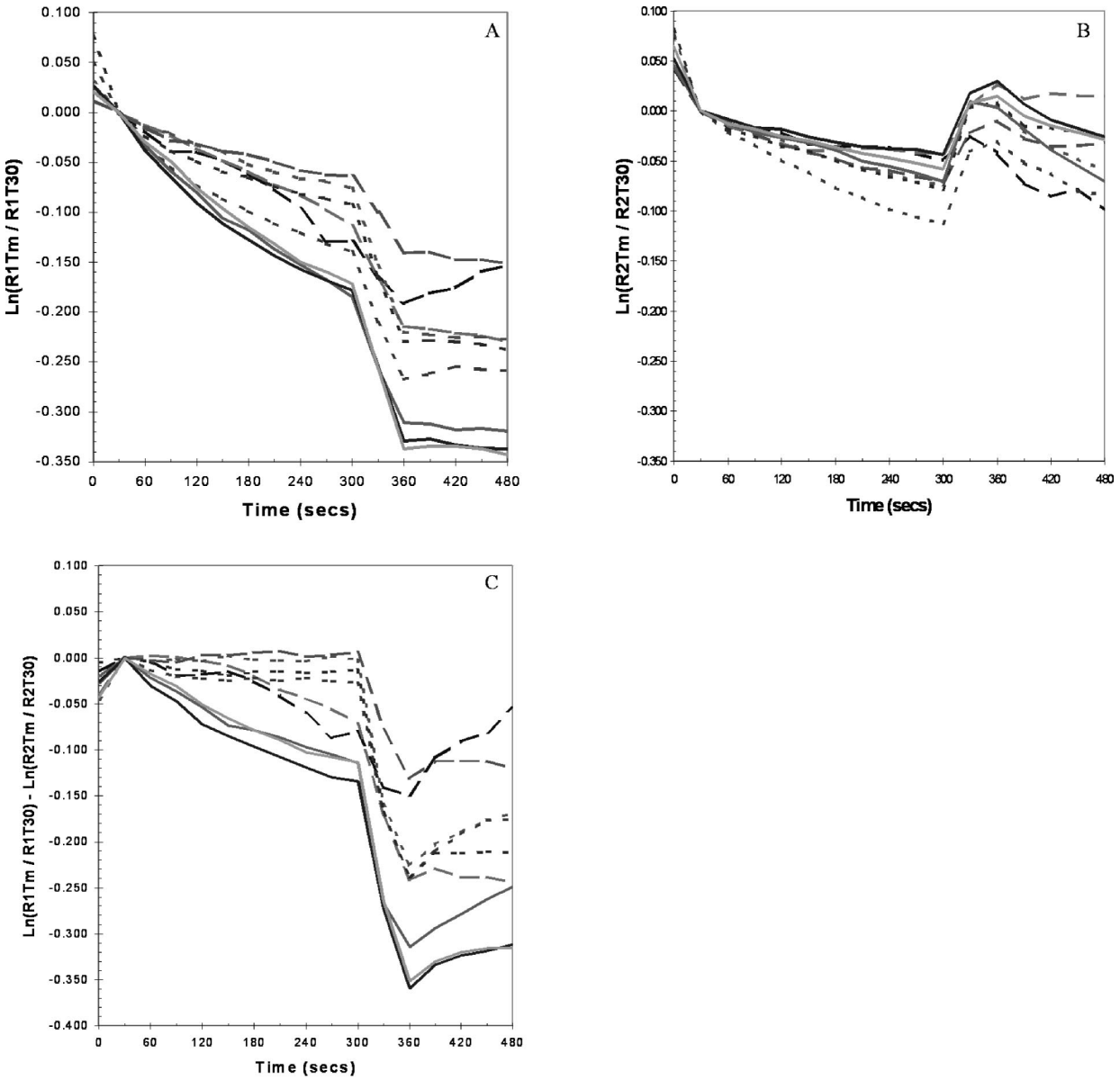

Fig. 4 (A) Thermo-optical differential response at 660 nm at one site of the skin plotted as the temperature-induced fractional change in localized reflectance $\{\ln[(R_{A1\,Tm}/R_{A1\,T30})]\}$ versus probe–skin contact time. The source–detector distance is 0.90 mm. Temperature perturbation of the optical probe at this site was changed from 38 to 22 °C. The dashed lines are data from diabetic subjects. The solid lines are data from nondiabetic subjects. (B) A plot similar to that of Fig. 4(A) but the temperature perturbation of the optical probe at this site was changed from cooling at 22 °C to heating to 38 °C. The dashed lines are data from diabetic subjects. The solid lines are data from nondiabetic subjects. (C) Thermo-optical differential response at 660 nm plotted as differences in the temperature-induced fractional change in localized reflectance $[\ln(R_{A1\,Tm}/R_{A1\,T30}) - \ln(R_{A2\,Tm}/R_{A2\,T30})]$ versus probe–skin contact time. The graph is plotted from the data in Figs. 4(A) and 4(B). The dashed lines are data from diabetic subjects. The solid lines are data from nondiabetic subjects. Each subject was measured three times.

diabetes duration of 2–15 years volunteered for the experiment. The subject's disease status was determined as diabetic or nondiabetic by previous diagnoses. Two data sets were collected, a training set and a prediction set. The training set consisted of four diabetic and four nondiabetic subjects, each tested six times (for a total of 48 data points). Measurements for the training set were performed at the time slots given in Table 1. These time slots were selected to cover different times during the day to allow the inclusion of several blood glucose concentrations and physiological and circadian rhythm conditions in the training set. The independent prediction set consisted of six diabetic and six nondiabetic subjects, each tested twice (a total of twenty-four data points). Measurement times for the prediction set were randomly chosen within a week.

Each subject sat in a clinical chair with the left forearm resting on the cradle. Prior to each measurement, the subject retracted the spring-loaded optical probe with the right hand, started a countdown to zero, then released the probe to contact the skin. Simultaneously, the operator initiated the temperature perturbation and data collection program. After completion of the test, the subject removed his or her arm from the

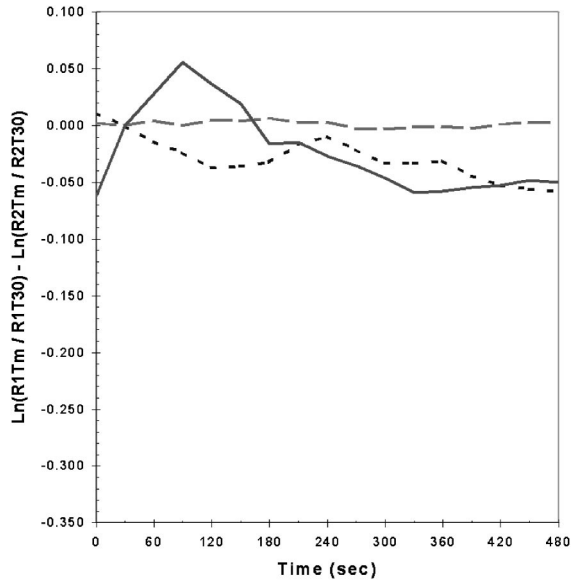

Fig. 5 Thermo-optical differential response at 660 nm plotted as $[\ln(R_{A1Tm}/R_{A1T30}) - \ln(R_{A2Tm}/R_{A2T30})]$ versus probe–skin contact time, for a source–detector distance of 0.90 mm. Both sites were heated and then cooled; therefore the temperatures of two probes are the same at any time point. The dashed lines are data from two diabetic subjects. The solid line is for a nondiabetic subject.

cradle. The steps were repeated for the second programmed temperature perturbation.

Three sets of temperature perturbation programs were used and are illustrated in Figs. 7(A), 7(B), and 7(C). In the first experiment, the probe at site 1 on the skin was maintained at 34 °C for 30 s and then lowered to 22 °C at a rate of 4 °C per minute, which required 180 s. The probe at site 2 was maintained at 34 °C for the 240 s of the measurement.

In the second experiment, site 1 on the skin was maintained at 38 °C for 30 s and then lowered to 22 °C at 5.33 °C per minute, which required 180 s. Site 2 was maintained at 22 °C for 30 s and then raised to 38 °C at 5.33 °C per minute.

In the third experiment, skin site 1 was maintained at 30 °C for 30 s and then cooled to 22 °C at a rate of 2.67 °C per minute over 180 s. Site 2 was treated in the opposite way; it was maintained at 30 °C for 30 s and then raised to 38 °C at 2.67 °C per minute.

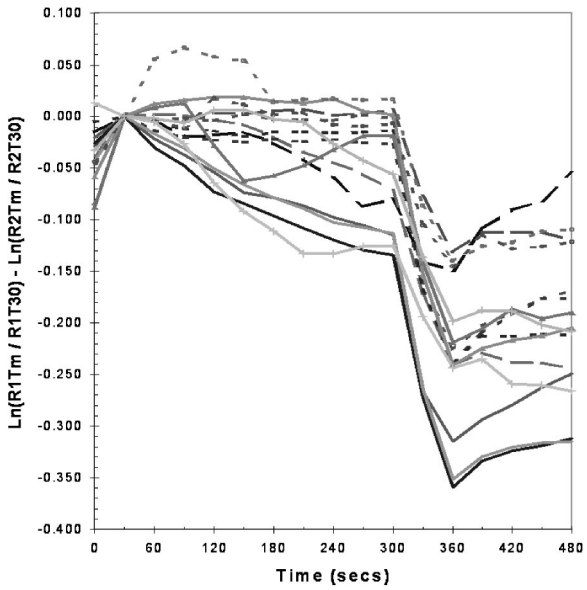

Fig. 6 Thermo-optical differential response at 660 nm plotted as $[\ln(R_{A1Tm}/R_{A1T30}) - \ln(R_{A2Tm}/R_{A2T30})]$ versus probe–skin contact time, for a source–detector distance of 0.90 mm. The data are normalized to the 30-s time point from initial probe–skin contact. The subjects include those whose data are plotted in Fig. 4(C) and additional ones with a different body mass index.

Table 1 Test times for the training and prediction sets.

Calibration Set	Test Set
8 subjects, each tested 6 times within 2 weeks	12 subjects each tested two times
1 Early morning, 8:00 to 10:00 a.m.	Two measurements taken at arbitrary time slots within a week.
2 Late morning, 10:00 to 11:00 a.m.	
3 Before lunch, 11:00 to 12:00 a.m.	
4 After lunch meal, 1:00 to 2:00 p.m.	
5 Mid-afternoon, 2:00 to 4:00 p.m.	
6 Late afternoon, after 4:00 p.m.	

4 Results and Discussion

4.1 *Qualitative Difference in Thermo-Optical Response of Diabetic Skin*

The natural log of the reflectance at the same site, for each wavelength and source–detector distance, was determined at two different temperatures to give $\ln\{R_{A1}(\lambda_i, r_j, T_l)/R_{A1}(\lambda_i, r_j, T_k)\}$ and then at the other site to give $\ln\{R_{A2}(\lambda_i, r_j, T_q)/R_{A2}(\lambda_i, r_j, T_p)\}$, representing the temperature-induced fractional change in reflectance at the first and second sites, respectively. These localized reflectance changes are simplified in the form $\ln[(R_{A1Tm}/R_{A1T30})]$ and $\ln[(R_{A2Tm}/R_{A2T30})]$. The reflectance value R_{A1Tm} is the localized reflectance at site 1 after m seconds of probe–skin contact for a particular wavelength and distance. R_{A1T30} is the localized reflectance at site 1 after 30 s of probe–skin contact. Similarly, R_{A2Tm} is the localized reflectance at site 2 after m seconds, and R_{A2T30} is the localized reflectance at site 2 after 30 s of probe–skin contact.

Figure 4(A) shows the temperature-induced fractional change in localized reflectance plotted as $\ln[(R_{A1Tm}/R_{A1T30})]$ versus probe–skin contact time at a single source–detector distance of 0.9 mm and at 660 nm. The plot represents the thermo-optical response at a site on the skin. The data are for two diabetic and one nondiabetic subject, each tested three times as described in the first experiment in Sec. 3.2.1. The temperature perturbation of the optical probe at the first area was changed from heating at 38 °C to cooling to 22 °C. There is an apparent separation of the temperature-induced localized reflectance signals generated by the diabetic subjects and those signals generated by the nondiabetic subject.

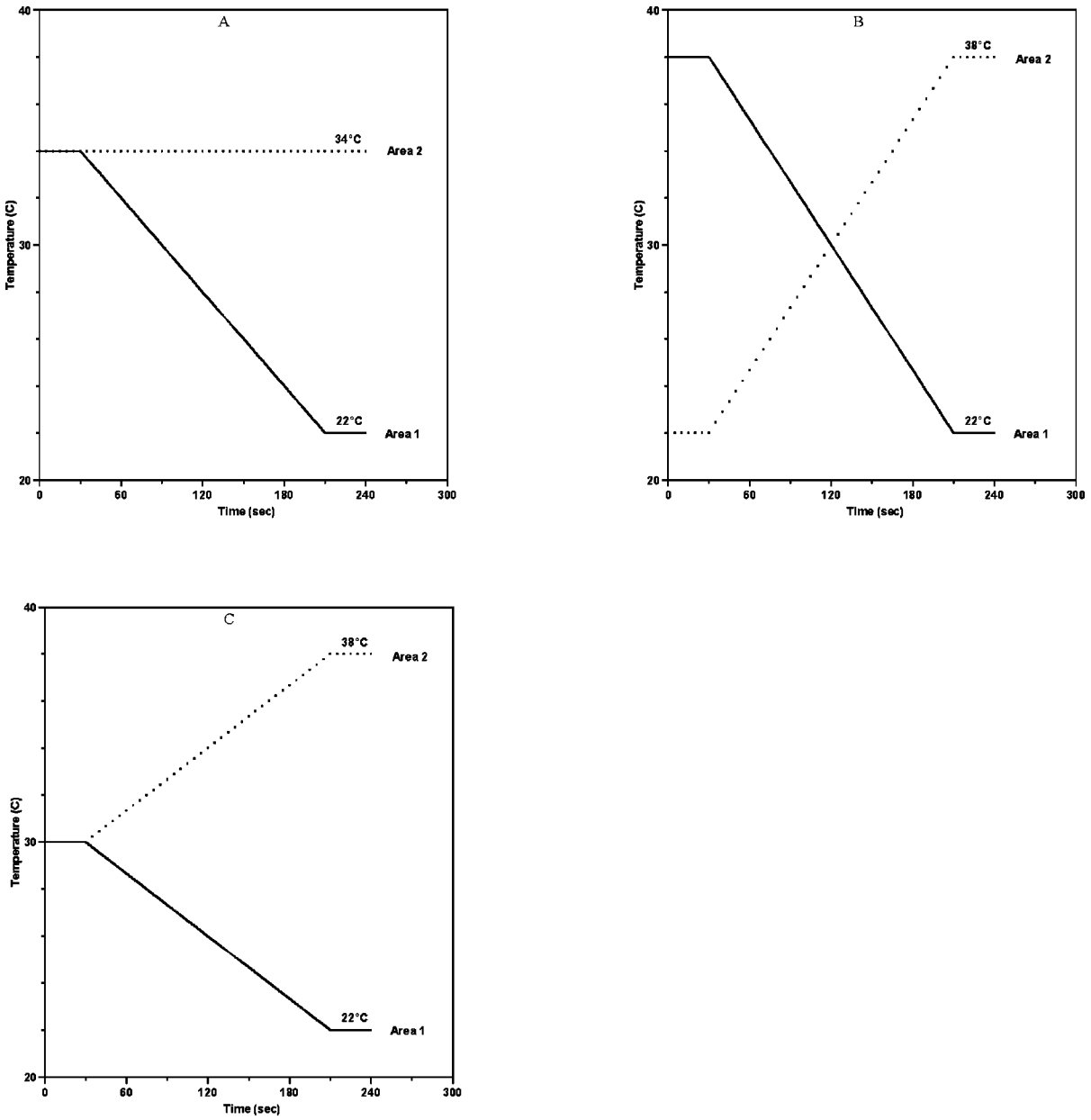

Fig. 7 (A) Temperature perturbation program corresponding to data in Table 3a. (B) Temperature perturbation program corresponding to data in Table 3b. (C) Temperature perturbation program corresponding to data in Table 3c.

Figure 4(B) shows a similar plot for the measurement at the second site, where the temperature change during the measurement was opposite to that applied for the case presented in Fig. 4(A). The temperature perturbation of the optical probe at this site was changed from cooling at 22 °C to heating to 38 °C. The separation between the signals generated by the diabetic subjects and those generated by the nondiabetic subject was less apparent.

Figure 4(C) shows a difference plot of the thermo-optical response curves. These are the differences in the temperature-induced localized reflectance change at site 1 and site 2; $[\ln(R_{A1Tm}/R_{A1T30}) - \ln(R_{A2Tm}/R_{A2T30})]$ plotted against probe–skin contact time. The data for this graph were calculated from the combined data in Fig. 4(A) and Fig. 4(B). For the cases presented in Fig. 4(A), Fig. 4(B), and Fig. 4(C), probe temperatures were different at each of the two sites at any comparable time point. A qualitative separation of diabetic and nondiabetic skin responses after a temperature change at 360 s in probe–skin contact is quite noticeable. The subtraction product ΔR_T, as expressed in Eq. (1), is the difference in the temperature-induced fractional change in localized reflectance at two skin sites, each subjected to a different temperature perturbation.

Figure 5 shows the thermo-optical differential response plots for the second experiment when the programmed temperature perturbation was the same at both sites. The experiment was performed on three subjects; two were diabetic and one was nondiabetic. The separation between the signals of the diabetics and the nondiabetic at the temperature inflection point at 360 s from probe–skin contact, which was noticeable

in Fig. 4(C), is not present in Fig. 5. The temperature response at the two sites is essentially the same, and a difference in temperature at the two sites is essential to the observed separation of the data between the diabetic and nondiabetic subjects.

The results for the third experiment, involving three additional volunteers of higher body mass (an index greater than 32), were also plotted. The qualitative separation between the plots of the temperature-induced fractional change in the localized reflectance $[\ln(R_{A1Tm}/R_{A1T30})-\ln(R_{A2Tm}/R_{A2T30})]$ versus the skin–probe contact time of the diabetic subject was also observed (not shown). When the seven nondiabetic (one subject tested three times and two subjects tested twice) and eight diabetic response curves (two subjects tested three times and one subject tested twice) were plotted together, some overlap between the response curves of the diabetic and nondiabetic subjects was observed, as shown in Fig. 6.

The qualitative separation of the thermo-optical response curves (temperature-induced fractional change in the localized reflectance versus time) for each body mass index group was also noticeable at 890 nm and a 0.9-mm source–detector distance. The separation was not as noticeable under the same programmed temperature change at other source–detector distances. It is then apparent that the use of a thermo-optical response at a single wavelength and at a single source–detector distance is not sufficient to overcome person-to-person differences in skin properties.

4.2 *Assessing the Relationship between a Temperature-Induced Localized Reflectance Change and Diabetic Status*

We used the two-site localized reflectance from multiple wavelengths and multiple source–detector distances in an attempt to separate the opto-thermal response of the skin of diabetic subjects from that of the nondiabetic subjects. The experimental protocol included the following improvements: (1) the number of subjects and the number of times they were tested was increased; and one portion of the data was used as a training set and another portion as a prediction set in a discriminant analysis approach; (2) all combinations of sixteen source–detector distances and wavelengths were incorporated; (3) different temperature limits were used; and (4) a nonlinear discriminant function was used as a classifier of the diabetic status instead of the visual inspection of graphs.

4.3 *Nonlinear Discriminant Functions for Data Analysis*

The difference in the temperature-induced fractional change in localized reflectance (ΔR_T) is expressed as a function f:

$$f(R_{A1t1},R_{At2},R_{A2t1},R_{A2t2})=[\ln(R_{A1t1}/R_{A1t2})]-[\ln(R_{A2t1}/R_{A2t2})], \quad (3)$$

where R_{A1t1} is the localized reflectance from skin site 1 at probe–skin contact time t_1, R_{A1t2} is the localized reflectance from site 1 at time t_2, R_{A2t1} is a localized reflectance from skin site 2 at time t_1, and R_{A2t2} is the same localized reflectance from site 2 at t_2. In this expression the contact time between the probe and the skin is used instead of the contact temperature. The temperature perturbation program employed at each site determines the cutaneous temperature at that site at any time point. The function f is applied to the optical signals at all source–detector distances and for all wavelengths.

The function(s) $f(R_{A1t1},R_{A1t2},R_{A2t1},R_{A2t2})$, determined at each of the four source–detector distances and at four wavelengths, together with the known diabetic or nondiabetic state of each subject in the training set, is used to generate a discriminant function D. A subject is classified as diabetic if $D>0$, and nondiabetic if $D<0$. D is a quadratic expression containing multiple functions of the type expressed in Eq. (3), and has the form:[33]

$$D=\sum_i \sum_j a_{ij}(\delta_i f_i)(\delta_j f_j)+\sum_i a_i\delta_i f_i+a_0, \quad (4)$$

where

$$\delta_i=1 \quad \text{or } 0; \quad \text{and } \sum_i \delta_i=K \quad (5a)$$

$$\delta_j=1 \quad \text{or } 0; \quad \text{and } \sum_j \delta_j=K, \quad (5b)$$

where a_{ij}, a_i, and a_0 are constants determined from the training set, and i or j are indices for specific combinations of wavelength and source–detector distance. The number K limits the total number of wavelength and source–detector distance combinations used in D to avoid overfitting; δ_i and δ_j were determined from the training set through a leave-one-out cross-validation procedure that minimizes the number of false classifications.

The true diabetic status of a subject was represented by S_i where $S_i=+1$ for a diabetic subject and $S_i=-1$ for a nondiabetic subject. D was calculated for each subject i as D_i. The subject is categorized as concordant if D_i and S_i had the same sign and was discordant if they had different signs. The coefficients of the quadratic function D of the calibration set were used to calculate the value of the function D_i for the

Table 2 Prediction of the diabetic status at 120 s after probe–skin contact.

Temperature Program #	Optical Test Result	True Status: Diabetic	True Status: Nondiabetic
1	Diabetic	11	3
	Nondiabetic	1	9
2	Diabetic	11[a]	1[a]
	Nondiabetic	0[a]	9[a]
3	Diabetic	10	0
	Nondiabetic	2	12

[a] Total number of data points is 24; 3 data points were rejected because they resulted in outlier optical signals.

Table 3a Performance parameters at different probe–skin contact times. Temperature perturbation steps correspond to those shown in Fig. 7(A).

Contact Time (seconds)	Probe Temperature (°C)		p	Sensitivity (%)	Specificity (%)	*PPV* (%)	*NPV*
	Site 1	Site 2					
120	34	28	0.0038	92	75	79	90
150	34	26	0.0011	92	83	85	91
180	34	24	0.0007	100	75	80	100
210	34	22	0.0011	83	92	91	85

Table 3b Performance parameters at different probe–skin contact times. Temperature perturbation steps correspond to those shown in Fig. 7(B).

Contact Time (seconds)	Probe Temperature (°C)		p	Sensitivity (%)	Specificity (%)	*PPV*	*NPV*
	Site 1	Site 2					
120	30	30	0.0001	92	90	92	100
150	27.3	32.7	0.0016	73	100	100	77
180	24.7	35.3	0.0004	90	90	90	90
210	22	38	0.0004	82	92	100	83

Table 3c Performance parameters at different probe–skin contact times. Temperature perturbation steps correspond to those shown in Fig. 7(C).

Contact Time (seconds)	Probe Temperature (°C)		p	Sensitivity (%)	Specificity (%)	*PPV*	*NPV*
	Site 1	Site 2					
120	26	34	0.0002	83	100	100	86
150	24.7	35.3	0.0011	92	83	85	91
180	23.3	36.7	0.0007	75	100	100	80
210	22	38	0.0002	100	83	86	100

prediction set. If $D_i > 0$, the subject was classified as diabetic. On the other hand, if $D_i < 0$, the subject was classified as nondiabetic.

The optical data points collected were divided into two classes, diabetic and nondiabetic subjects. A 2×2 prediction matrix $\begin{bmatrix} \alpha & \gamma \\ \chi & \beta \end{bmatrix}$ was established. Designating the number of true diabetics identified as "α," the number of true nondiabetics identified as "γ," the number of diabetic subjects identified as nondiabetic (false negative) as "χ," and the number of nondiabetics identified as diabetic (false positive classification) as "β," the sensitivity $= \alpha/(\alpha+\chi)$, specificity $= \gamma/(\gamma+\beta)$, positive predictive value $(PPV) = \alpha/(\alpha+\beta)$, and negative predictive value $(NPV) = \gamma/(\chi+\gamma)$ were calculated.

Classification was then attempted utilizing Eqs. (4), (5a), and (5b), and using optical signals at eight wavelength–distance combinations (i.e., $K=8$) at $t_1 = 30$ s and at any of these time points t_2: 120, 150, 180, and 210 s from the probe–skin contact. Prediction of the diabetic status using the three different temperature perturbation conditions and using the signal at 120 s from the onset of probe–skin contact is given in Table 2. The data in the table indicate that it was possible to achieve a separation between the diabetics and nondiabetics using the nonlinear discriminant function and eight distance–wavelength combinations, which was not consistently achievable at a single wavelength and a single source–detector distance.

Differentiation between diabetic and nondiabetic subjects was not sensitive to the contact time between the skin and the probe beyond 120 s, as shown for the first temperature perturbation program in Table 3a. Similar data were obtained for the two other temperature perturbation programs as shown in Tables 3b and 3c. The data presented in the three tables indicate that prediction of diabetic status was achievable at 120 s of probe–skin contact. The quality of the data was not appreciably enhanced by increasing the probe–skin contact times. The total time for each sequential measurements was less than 5 min. Furthermore, the classification was not limited to one unique programmed temperature perturbation. Any of the three temperature programs resulted in a separation of the test population into diabetic and nondiabetic subjects.

5 Conclusion

We describe a near-infrared optical method that assesses the diabetic status of human subjects by measuring the cutaneous localized reflectance under specific thermal perturbations and the use of a nonlinear discriminant function as a classifier. The method involves two sequential localized reflectance measurements under different temperature perturbations, each measurement lasting less than 300 s. An acceptable classification was achieved after 120 s of contact time for each measurement. The thermo-optical response of the skin's localized reflectance in diabetic subjects appears to differ from that of nondiabetic subjects.

It is possible to explain the observed differentiation in the thermo-optical response as due to a combination of:

1. the temperature dependence of absorption and scattering changes caused by red blood cell structural changes, differences in cell aggregation, and the refractive index
2. a change in temperature dependence in tissue scattering that is due to the effect of diabetes on cutaneous collagen fibers and subsequent differences in refractive index mismatches
3. a difference in microcirculation response to temperature change.

The use of a nonlinear discriminant function as a classifier did overcome person-to-person differences in skin optical properties and the variable glucose concentrations at the time of measurement. The preliminary data show a differentiation between the two populations in a limited number of subjects. A larger population is needed to test possible correlation with the values of glycated hemoglobin.

Monitoring the temperature-induced fractional change in the localized reflectance as presented in this paper demonstrated the ability to differentiate between diabetic and nondiabetic subjects in the population studied. Studies with larger populations that include subjects with impaired glucose tolerance, subjects with early diagnosed diabetes, and those with advanced diabetes are needed in order to improve the statistical predictability of the method and to relate the changes in signal to skin pathology and progress of the disease. A comparison with other vasodilatation induction methods, such as LDF accompanied by iontophoreses of acetylcholine or sodium nitroprusside, similar to those reported in Ref. 27, will help separate the circulation effects from the structural effects on the classification.

Acknowledgments

The authors thank Dr. John Lindberg and Dr. Arnold Stalder for optics design. We acknowledge the effort of Ron Hohs in electronic design, James Forsyth in equipment fabrication, Steve Kuchenbrod in data collection, Brenda Calfin for the Institutional Review Board documentation, and Michael Lowery and Eric Shain for graphical help. We also thank Drs. Vickey Blakesley and Mike Jirousek, Abbott Laboratories Global Pharmacuetical Research and Development, for helpful discussions on diabetes complications.

References

1. O. Khalil, "Spectroscopic and clinical aspects of noninvasive glucose measurements," *Clin. Chem.* **45**, 165–177 (1999).
2. M. R. Robinson, R. P. Eaton, D. M. Haaland, G. W. Keep, E. V. Thomas, B. R. Stalled, and P. L. Robinson, "Noninvasive glucose monitoring in diabetic patients: a preliminary evaluation," *Clin. Chem.* **38**, 1618–1622 (1992).
3. K. U. Jagemann, C. Fischbacher, K. Danzer, U. A. Muller, and B. Mertes, "Application of near-infrared spectroscopy for noninvasive determination of blood/tissue glucose using neural network," *Z Phys. Chem.* **191S**, 179–190 (1995).
4. N. Wiernsperger, "Defects in microvascular haemodynamics during prediabetes: Contributor or epiphenomenon?" *Diabetologia* **43**, 1439–1449 (2000).
5. S. B. Wilson, "Detection of microvascular impairment in type 1 diabetes by laser Doppler flowmetry," *Clin Phys.* **12**, 195–208 (1992).
6. M. Rendell, T. Bergman, G. O'Donnell, E. Drobny, J. Borgos, and R. Bonnor, "Microvascular blood flow, volume, and velocity, measured by laser Doppler techniques in IDDM," *Diabetes* **38**, 819–824 (1989).
7. M. Rendell and O. Bamisedun, "Diabetic cutaneous microangiopathy," *Am. J. Med.* **93**, 611–618 (1992).
8. I. M. Braverman and A. Keh-Yen, "Ultrastructural abnormalities of the microvasculature and elastic fibers in the skin of juvenile diabetics," *J. Invest. Dermatol.* **82**, 270–274 (1984).
9. G. Rayman, S. A. Williams, P. D. Spenser, L. H. Smajie, P. H. Wise,

and J. E. Tooke, ''Impaired microvascular hyperemic response to minor skin trauma in type 1 diabetes,'' *Br. Med. J.* **292**, 1295–1298 (1986).
10. F. Khan, T. Elhadd, S. A. Green, and J. Belch, ''Impaired skin microvascular function in children, adolescent, and young adults with type 1 diabetes,'' *Diabetes Care* **23**, 215–220 (2000).
11. J. E. Tooke, J. Ostergren, P-E. Lins, and B. Fragrell, ''Skin microvascular blood flow control in long duration diabetics with and without complications,'' *Diabetes Res.* **5**, 189–192 (1987).
12. D. D. Sandeman, A. C. Shore, and J. E. Tooke, ''Relation of skin capillary pressure in patients with insulin-dependent diabetes mellitus to complications and metabolic control,'' *New Engl. J. Med.* **327**, 760–764 (1992).
13. A. J. Jaap, M. S. Hammersley, A. C. Shore, and J. E. Tooke, ''Reduced microvascular hyperemia in subjects at risk of developing Type 2 (non-insulin-dependent) diabetes mellitus,'' *Diabetologia* **37**, 214–216 (1994).
14. K. B. Stansberry, S. A. Shapiro, M. A. Hill, P. M. McNitt, M. D. Meyer, and A. I. Vinik, ''Impaired peripheral vasomotion in diabetes,'' *Diabetes Care* **19**, 715–721 (1996).
15. E. Haak, T. Haak, Y. Grozinger, G. Krebs, K. H. Usadel, and K. Kusterer, ''The impact of contralateral cooling of skin capillary blood cell velocity in patients with diabetes mellitus,'' *J. Vasc. Res.* **35**, 245–249 (1998).
16. J. E. Tooke, P. E. Lins, J. Ostergren, and B. Fagrell, ''Skin microvascular autoregulatory response in Type 1 diabetics: the influence of duration and control,'' *Int. J. Microcirc.: Clin. Exp.* **4**, 249–256 (1985).
17. S. J. Benbow, D. W. Pryce, K. Noblett, I. A. Macfarline, P. S. Friedman, and G. Williams, ''Flow motion in peripheral diabetic neuropathy,'' *Clin. Chem.* **88**, 191–196 (1995).
18. R. G. Sibbald, S. J. Landolt, and D. Toth, ''Skin and diabetes,'' *Endocrinol. Metabol. Clinics N. Am.* **25**, 463–472 (1996).
19. V. M. Monnier, O. Bautista, D. Kenny, D. R. Sell, J. Fogarty, W. Dahms, P. A. Cleary, J. Lachin, and S. Genuth, ''Skin collagen glycation, glycoxidation, and crosslinking are lower in subjects with long-term intensive versus conventional therapy of type 1 diabetes: relevance of glycated collagen products versus HbA1c as markers for diabetic complications,'' *Diabetes* **48**, 870–880 (1999).
20. V. J. James, L. Belbridge, S. V. McLennan, and D. K. Yue, ''Use of X-ray diffraction in study of human diabetic and aging collagen,'' *Diabetes* **40**, 391–394 (1991).
21. S-j. Yeh, O. S. Khalil, C. F. Hanna, S. Kantor, X. Wu, T-W. Jeng, and R. A. Bolt, ''Temperature dependence of optical properties of *in-vivo* human skin,'' *Optical Tomography and Spectroscopy of Tissue IV*, Britton Chance, Ed., *Proc. SPIE* **4250**, 455–461 (2001).
22. O. S. Khalil, S-j. Yeh, M. G. Lowery, X. Wu, C. F. Hanna, S. Kantor, T-W. Jeng, J. Kanger, R. A. Bolt, and F. F. de Mul, ''Temperature modulation of optical properties of human skin,'' *J. Biomed. Opt.* **8**, 191–205 (2003).
23. J. Laufer, R. Simpson, M. Kohl, M. Essenpreis, and M. Cope, ''Effect of temperature on the optical properties of *ex vivo* human dermis and subdermis,'' *Phys. Med. Biol.* **43**, 2479–2489 (1998).
24. X. Wu, S-j. Yeh, T-W. Jeng, and O. S. Khalil, ''Noninvasive determination of hemoglobin and hematocrit using a temperature-controlled localized reflectance tissue photometer,'' *Anal. Biochem.* **287**, 284–293 (2000).
25. T. J. Farrell, M. S. Patterson, and B. C. Wilson, ''A diffusion theory model of spatially resolved, steady-state diffuse reflectance for the noninvasive determination of tissue optical properties *in vivo*,'' *Med. Phys.* **19**, 879–888 (1992).
26. K. B. Stansberry, M. A. Hill, S. A. Shapiro, P. M. McNitt, B. A. Bhatt, and A. I. Vinik, ''Impairment of peripheral blood flow response in diabetes resembles enhanced aging effects,'' *Diabetes Care* **20**, 1711–1719 (1997).
27. A. E. Caballero, S. Arora, R. Saouaf, S. C. Lim, P. Smakowski, J. Y. Park, G. L. King, F. W. LoGerfo, E. S. Horton, and A. Veves, ''Microvascular and macrovascular reactivity is reduced in subjects at risk for type 2 diabetes,'' *Diabetes* **48**, 1856–1862 (1999).
28. N. N. Firsov, A. V. Priezzhev, O. M. Ryaboshapka, and I. V. Sirko, ''Aggregation and disaggregation of erythrocytes in whole blood: study by backscattering technique,'' *J. Biomed. Opt.* **4**, 76–84 (1999).
29. Y. I. Gurfinkel, K. V. Ovsyannikov, A. S. Ametov, I. A. Strokov, and A. Priezzhev, ''Early diagnosis of diabetes mellitus using noninvasive imaging by computer capillaroscopy,'' in *Technical Digest*, Optical Society of America Biomedical Topical Meetings, Miami Beach, FL, April 7–10, Paper Su-D4-1, pp. 62–64 (2002).
30. L. D. Shvartsman and I. Fine, ''RBC Aggregation effects on light scattering from blood,'' in *Controlling Tissue Optical Properties: Application in Clinical Study*, Valery Tuchin, Ed., *Proc. SPIE* **2162**, 120–129 (2000).
31. G. Mazarevica, T. Freivalds, and A. Jurka, ''Properties of erythrocyte light refraction in diabetic patients,'' *J. Biomed. Opt.* **7**, 244–247 (2002).
32. R. Graaff, J. G. Aarnoudse, J. R. Zijp, P. M. A. Sloot, F. F. de Mul, J. Greve, and M. H. Koelink, ''Reduced light-scattering properties for mixtures of spherical particles: a simple approximation derived from Mie calculations,'' *Appl. Opt.* **31**, 1370–1376 (1992).
33. R. O. Duda, P. E. Hart, and D. G. Stork, *Pattern Classification*, 2nd ed., pp. 215–225, Wiley, New York (2001).